

Parameter estimation from an Ornstein-Uhlenbeck process with measurement noise

Simon Carter

*Applied Mathematics and Laufer Center for Physical and Quantitative Biology,
Stony Brook University, Stony Brook NY 11794-5281.*

Helmut H. Strey

*Biomedical Engineering Department and Laufer Center for Physical and Quantitative Biology,
Stony Brook University, Stony Brook NY 11794-5281.*

(Dated: August 7, 2023)

This article aims to investigate the impact of noise on parameter fitting for an Ornstein-Uhlenbeck process, focusing on the effects of multiplicative and thermal noise on the accuracy of signal separation. To address these issues, we propose algorithms and methods that can effectively distinguish between thermal and multiplicative noise and improve the precision of parameter estimation for optimal data analysis. Specifically, we explore the impact of both multiplicative and thermal noise on the obfuscation of the actual signal and propose methods to resolve them. Firstly, we present an algorithm that can effectively separate thermal noise with comparable performance to Hamilton Monte Carlo (HMC) but with significantly improved speed. Subsequently, we analyze multiplicative noise and demonstrate that HMC is insufficient for isolating thermal and multiplicative noise. However, we show that, with additional knowledge of the ratio between thermal and multiplicative noise, we can accurately distinguish between the two types of noise when provided with a sufficiently large sampling rate or an amplitude of multiplicative noise smaller than thermal noise. This finding results in a situation that initially seems counter intuitive. When multiplicative noise dominates the noise spectrum, we can successfully estimate the parameters for such systems after adding additional white noise to shift the noise balance.

A. Introduction

Parameter estimation from data is a critical aspect of statistical modeling and machine learning. It enables the determination of the ideal values for the parameters of a model given observation data, and accurate parameter estimation is essential for obtaining meaningful results from a model [1]. Additionally, incorporating prior knowledge and constraints into the estimation process allows for a more robust and interpretable model, at the cost of the accuracy of those assumptions [2]. Moreover, the estimation process helps to identify patterns and relationships in the data and make predictions based on those patterns [1]. Methods for parameter estimation from stochastic differential equations are reviewed in [3].

The Ornstein-Uhlenbeck (OU) process [4] is a widely used and important mathematical tool for modeling and understanding various real-world phenomena. It has been widely studied in physics, finance, biology, neuroscience, and engineering. The OU process is a continuous-time Markov process characterized by its mean-reverting behavior towards a long-term average. This makes it well-suited for modeling situations where there is a tendency for a variable to return to a long-term average, while also allowing for short-term fluctuations. The OU process has been used in finance to model the dynamics of stock prices and interest rates [5], in biology to model the evolution of population sizes [6], in neuroscience to model neural activity [7, 8], and in engineering to model the behavior of control systems [9]. Previously we had developed an analytical solution for the maximum likelihood parameter fitting of an Ornstein-Uhlenbeck process without measurement noise [10].

Measurement noise is a ubiquitous issue in parameter estimation from data, and it can significantly impact the accuracy and reliability of the estimated parameters. Measurement noise refers to the inaccuracies and fluctuations in the measurement process that result in data points that deviate from the true underlying relationship [11]. The presence of measurement noise can obscure the true patterns and relationships in the data, making it more challenging to estimate the parameters of a model accurately [1]. Moreover, measurement noise can also increase the variability of the data, leading to increased uncertainty in the estimated parameters. This can result in less precise and unreliable estimates and increase the risk of overfitting the data, where the model fits the measurement noise rather than the true underlying relationship.

The challenge of noise removal has been explored in many different aspects traditionally managed through filtering or averaging. Here we present a Bayesian approach that models the data and the noise probabilistically and simultaneously. Specifically, we look at two types of noise, additive Gaussian (white) and signal dependant (multiplicative) noise. White noise is the most commonly modeled and assumed noise. However, in many cases, signal-dependent noise can be the dominant source of noise, with the most prominent examples found in computer vision and neuronal

models. An approximation of this signal-dependent noise as white noise may not be sufficient. [12, 13]

In this paper, we introduce methods for parameter fitting of an Ornstein-Uhlenbeck (OU) process with added white noise, as well as a combination of white noise and multiplicative noise. For the case of white noise alone, we developed an expectation-maximization algorithm that estimates the parameters from data. Our method returns parameter values that are similar to those obtained using more general Hamilton Monte Carlo (HMC) methods but is computationally more efficient. When multiplicative noise is added to an OU process (signal), even HMC methods cannot adequately separate the noise from the signal. This is likely due to the similarity between the powerspectra of the multiplicative noise and the signal. We found that the OU signal parameters, as well as the amplitudes of the white noise and multiplicative noise, can be estimated using probabilistic modeling if the ratio of multiplicative to white noise does not exceed a threshold that depends on the sampling rate of the data. We concluded that, to successfully model a mixture of white and multiplicative noise, the ratio of white to multiplicative noise must be known.

B. Probabilistic Description of Processes

A probabilistic description of an overdamped Brownian particle in a harmonic potential (also called the Ornstein-Uhlenbeck process) was first reported by Ornstein and Uhlenbeck in 1930 [4]

$$x_{t+\Delta t} \sim \mathcal{N}(\mu = Bx_t, \sigma^2 = A(1 - B^2)) \quad (1)$$

where $B(\Delta t) = \exp(-\frac{\Delta t}{\tau})$ with τ as the relaxation time, and \mathcal{N} representing a normal distribution. This equation describes the conditional probability of finding a particle at time $t + \Delta t$ at $x_{t+\Delta t}$ given that it was at x_t at time t . The likelihood function for a specific time trace, that is taken at intervals Δt , $\{x_i(i\Delta t)\}$ is:

$$p(\{x_i(t_i)\} | B, A) = \frac{1}{\sqrt{2\pi A}} \exp\left(-\frac{x_1^2}{2A}\right) \frac{1}{\sqrt{2\pi A(1 - B^2(\Delta t))}^{(N-1)}} \times \exp\left(-\sum_{i=1}^{N-1} \frac{(x_{i+1} - x_i B(\Delta t))^2}{2A(1 - B^2(\Delta t))}\right) \quad (2)$$

We recently published an analytical solution to the Ornstein-Uhlenbeck maximum likelihood problem [10] and here we want to consider the same problem but with added noise. Here we will consider Gaussian white noise with variance σ_N^2 and multiplicative noise $\sigma_M^2 x^2(t)$ that is added to each data point. The two noise sources can be described as follows:

$$y_i \sim \mathcal{N}(\mu = x_i, \sigma^2 = \sigma_N^2 + \sigma_M^2 x_i^2) \quad (3)$$

with likelihood function for the measured data $\{y_i\}$ given $\{x_i\}$ and σ_N :

$$p(\{y_i(t_i)\} | \{x_i(t_i)\}, \sigma_N) = \frac{1}{\sqrt{2\pi\sigma_N^2}^N} \exp\left(-\sum_{i=1}^N \frac{(y_i - x_i B(\Delta t))^2}{2(\sigma_N^2 + \sigma_M^2 x_i^2)}\right) \quad (4)$$

Since we are measuring $\{y_i\}$, $\{x_i\}$ are latent variables. If we knew $\{x_i\}$ and $\{y_i\}$ the likelihood function would simply be.

$$p(\{x_i\}, \{y_i\} | A, B, \sigma_N) = p(\{y_i(t_i)\} | \{x_i(t_i)\}, \sigma_N) p(\{x_i(t_i)\} | B, A) \quad (5)$$

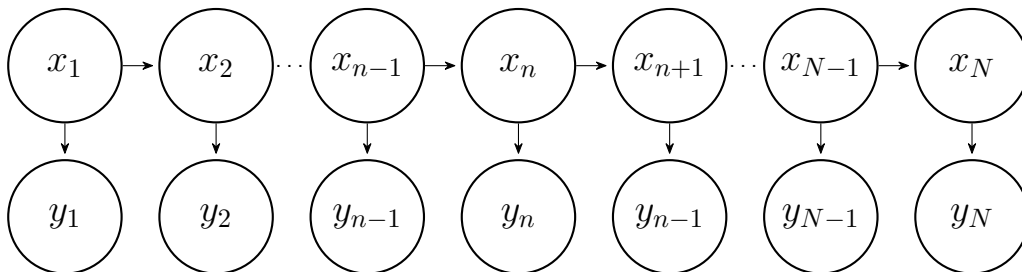


FIG. 1: Graph representation of a chain of N values $\{x_i\}$ that originate from an OU process with corresponding $\{y_i\}$ that represent the measured values containing noise

But since we don't observe $\{x_i\}$, we need to marginalize over $\{x_i\}$:

$$p(\{y_i\}|A, B, \sigma_N, \sigma_M) = \int \cdots \int p(\{x_i\}, \{y_i\}|A, B, \sigma_N, \sigma_M) dx_1 \dots dx_N \quad (6)$$

Using Bayes Theorem, we can express the conditional probability of the parameters $\{A, B, \sigma_N, \sigma_M\}$ given the measured data $\{y_i\}$.

$$p(\{A, B, \sigma_N, \sigma_M\}|\{y_i\},) \propto p(\{y_i\}|A, B, \sigma_N) p(A, B, \sigma_N, \sigma_M) \quad (7)$$

In principle, from this equation, we could estimate the parameters from a measurement of $\{y_i\}$ using a maximum likelihood approach.

I. EXPECTATION MAXIMIZATION ALGORITHM FOR THERMAL NOISE

As we can see from the previous equation, a simple maximum likelihood approach is computationally challenging. Because we are dealing with Gaussian distributions, a typical approach is to take the logarithm of the likelihood and hope that the likelihood factors nicely. But in our case, because of the marginalization of the hidden variables $\{x_i\}$, we are taking the logarithm of integrals over $\{x_i\}$ which does not simplify the equation. On the other hand, we recognize that $p(\{x_i\}, \{y_i\}|A, B, \sigma_N)$ factors nicely. The Expectation Maximization (EM) algorithm takes advantage of this fact (see [2] chapter 9). The EM algorithm works as follows: (1) pick a starting point for the parameters $\Theta^{old} = \{A^{old}, B^{old}, \sigma_N^{old}\}$; (2) calculate the probability distribution for each hidden variable $\{x_i\}$ given these parameters; (3) maximize the following function concerning Θ to find the new parameters.

$$\mathcal{Q}(\Theta, \Theta^{old}) = \int \cdots \int p(\{x_i\}|\{y_i\}, \Theta^{old}) \ln p(\{x_i\}, \{y_i\}|\Theta) dx_1 \dots dx_N \quad (8)$$

(4) repeat by using Θ as Θ_{old} until convergence. The EM algorithm converges, but it may find local maxima in the posterior distribution. Therefore it is important to vary the starting point for Θ . To evaluate the integral in eq 8, we need to calculate $p(x_n|\{y_i\}, \Theta^{old})$. We can again use Bayes rule and the conditional Independence rules of a linear hidden Markov chain:

$$\begin{aligned} p(x_n|\{y_i\}, \Theta^{old}) &= \frac{p(\{y_i\}|x_n, \Theta^{old}) p(x_n)}{p(\{y_i\}|\Theta^{old})} \\ &= \frac{p(y_1, \dots, y_n|x_n, \Theta^{old}) p(y_{n+1}, \dots, y_N|x_n, \Theta^{old}) p(x_n)}{p(\{y_i\}|\Theta^{old})} \\ &= \frac{p(y_1, \dots, y_n, x_n|\Theta^{old}) p(y_{n+1}, \dots, y_N|x_n, \Theta^{old})}{p(\{y_i\}|\Theta^{old})} \\ &= \frac{\alpha(x_n) \beta(x_n)}{p(\{y_i\}|\Theta^{old})} \end{aligned} \quad (9)$$

using the following definition

$$\begin{aligned} \alpha(x_n) &= p(y_1, \dots, y_n, x_n|\Theta^{old}) \\ \beta(x_n) &= p(y_{n+1}, \dots, y_N|x_n, \Theta^{old}) \end{aligned} \quad (10)$$

here we took advantage of the properties of the Markov chain $\{x_i\}$. If we know a specific x_n then x_{n-1} and x_{n+1} are independent because the path between the two is blocked (See for example [2]). As a consequence of that, the y_i with $i \leq n$ are independent of y_i with $i > n$ conditioned on x_n . Both $\alpha(x_n)$ and $\beta(x_n)$ can be defined and calculated recursively:

$$\begin{aligned} \alpha(x_n) &= p(y_n|x_n, \Theta^{old}) \int \alpha(x_{n-1}) p(x_n|x_{n-1}, \Theta^{old}) dx_{n-1} \\ \beta(x_n) &= \int \beta(x_{n+1}) p(y_{n+1}|x_{n+1}, \Theta^{old}) p(x_{n+1}|x_n, \Theta^{old}) dx_{n+1} \end{aligned} \quad (11)$$

with the starting value of

$$\begin{aligned}\alpha(x_1) &\propto \exp\left(-\frac{x_1^2}{2A}\right) \exp\left(-\frac{(y_1 - x_1)^2}{2\sigma_N^2}\right) \\ \beta(x_N) &= 1\end{aligned}\tag{12}$$

Here we have to notice that all probability distributions are Gaussian, which means that the product of two Gaussians as well as the convolution of two Gaussians is also a Gaussian. As a consequence, all $\alpha(x_n)$ and $\beta(x_n)$ are Gaussian (except for $\beta(x_N)$). For a computation, all we need to calculate is the mean and standard deviation of each $\alpha(x_n)$ and $\beta(x_n)$ since the normalization of Gaussians is known. Similarly, we can calculate the probability distributions of consecutive x_{n-1} and x_n :

$$\begin{aligned}p(x_{n-1}, x_n | \{y_i\}, \Theta^{old}) &= \frac{p(\{y_i\} | x_{n-1}, x_n, \Theta^{old}) p(x_{n-1}, x_n)}{p(\{y_i\} | \Theta^{old})} \\ &= \frac{p(y_1, \dots, y_n | x_n, \Theta^{old}) p(y_{n+1}, \dots, y_N | x_n, \Theta^{old}) p(x_n)}{p(\{y_i\} | \Theta^{old})} \\ &= \frac{\alpha(x_{n-1}) p(y_n | x_n, \Theta^{old}) p(x_n | x_{n-1}, \Theta^{old}) \beta(x_n)}{p(\{y_i\} | \Theta^{old})}\end{aligned}\tag{13}$$

We can now move to the implementation of the EM algorithm for our specific case: (1) We pick starting values for the parameters A, B, σ_N ; (2) We calculate all $p(x_n | \{y_i\}, \Theta^{old})$ and $p(x_{n-1}, x_n | \{y_i\}, \Theta^{old})$ which represent the E step; (3) We calculate the improved parameters by using the procedure for estimating parameters from an OU process without additional measurement noise [10], which yields improved parameters for A and B . For this analysis we only require the expectation values of x_1^2, x_N^2 , the sum of x_i^2 , and $x_i x_{i+1}$ which can be calculated using eq.9 and eq.13. The updated value for σ_N can be obtained by considering the following:

$$\ln \prod_{i=1}^N \frac{1}{\sqrt{2\pi\sigma_N^2}} \exp\left(-\frac{(x_i - y_i)^2}{2\sigma_N^2}\right) = -N \ln \sigma_N - \frac{1}{2\sigma_N^2} \sum_{i=1}^N (x_i - y_i)^2\tag{14}$$

The maximum of this expression can be found by setting its derivative with respect to σ_N to zero, which results in:

$$\sigma_{N,max}^2 = \frac{1}{N} \sum_{i=1}^N \sigma_{x_i}^2 + \mu_{x_i}^2 + y_i^2 - 2\mu_{x_i} y_i\tag{15}$$

where we use the σ_{x_i} and μ_{x_i} from $p(x_n | \{y_i\}, \Theta^{old}) = \mathcal{N}(x_i, \mu = \mu_{x_i}, \sigma = \sigma_{x_i})$.

To determine the error of the estimated parameters after convergence of the EM algorithm, we can take advantage of the fact that when the EM algorithm has converged then $\mathcal{Q}(\Theta, \Theta^{old})$ is equal to the posterior distribution [2] and we can use the error estimates for A and B from [10]. Since σ_N is independent from A and B in $\mathcal{Q}(\Theta, \Theta^{old})$, we can write:

$$d\sigma_{N,max} = \frac{\sigma_{N,max}}{\sqrt{2N}}\tag{16}$$

We validated our EM algorithm against Hamilton Monte-Carlo (HMC) methods using simulated ground truth OU time series with known parameters ($A = 1$, and $\tau = 1$). Any of our results can be applied to any parameter combination by rescaling the parameters. Hamilton MC methods are drawing samples directly from the posterior distribution and therefore provide accurate estimations of the parameters and their uncertainties. Specifically, we implemented the HMC methods in the Julia programming language [14] using the probabilistic programming package Turing.jl [15]. We obtained 1000 samples per data point employing the NUTS sampler [16]. The EM method outperforms the HMC method consistently by a factor of 100 using the same computer configuration. Fig. 2 illustrates that even though the EM method obtains the same parameter estimates, it severely underestimates their uncertainties. This is not surprising, since in EM the uncertainty is estimated by assuming a posterior distribution with a Normal distribution. In our earlier paper on parameter estimation of OU processes without measurement noise, we found that the maximum likelihood method similarly underestimated the uncertainty of the parameters by about a factor of five [10].

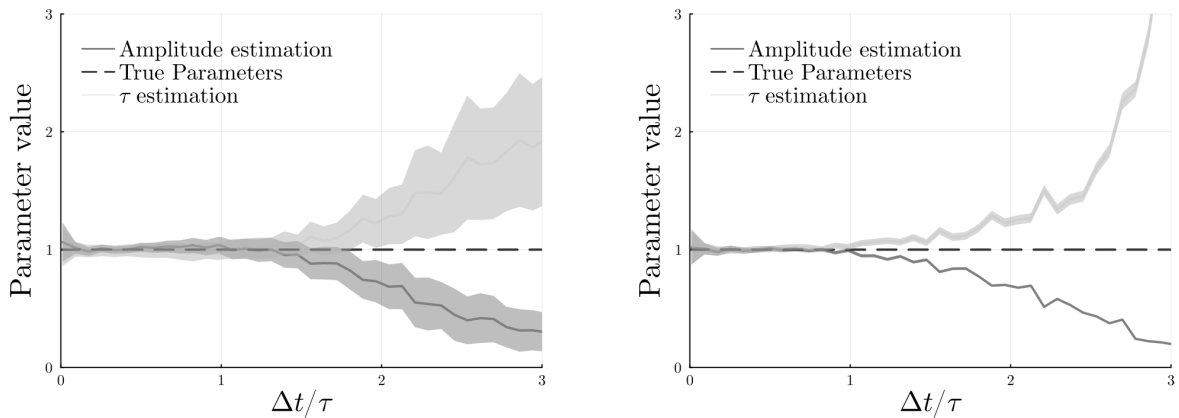


FIG. 2: The parameter estimation as a function of the sample rate. The left graph was generated using traditional HMC and the right graph was generated using our EM algorithm. The ribbon around each is the standard deviation of the estimate, and for both parameters, the true values are equal to 1 (dashed line)

II. PROPERTIES OF MULTIPLICATIVE NOISE

In this section, we investigate the characteristics of multiplicative noise as defined by the parameter σ_M in equation 3. Compared to additive noise, multiplicative noise is more challenging to distinguish from the signal, and traditional methods such as Hamilton Monte Carlo (HMC) fail to sample the posterior distribution effectively. This limitation can be explained by examining the power spectrum of the signal. Specifically, the first-order power spectrum shows that both thermal and multiplicative noise appear identical and uncorrelated, which could lead to the incorrect conclusion that both types of noise can be removed easily and treated similarly. However, upon examining higher-order spectra of the signals, a clear separation between thermal and multiplicative noise emerges, highlighting the difficulties of accurately separating and modeling multiplicative noise. We can start to examine this relationship by defining the fourth-order correlation function

$$g_y^2(t_1, t_2) = \langle y_{t_1}^2 y_{t_2}^2 \rangle = E[y_{t_1}^2 y_{t_2}^2] = \int_{-\infty}^{\infty} \int_{-\infty}^{\infty} y_{t_1}^2 y_{t_2}^2 \rho(y_{t_1}, y_{t_2}) dy_{t_1} dy_{t_2} \quad (17)$$

Here y_{t_1} and y_{t_2} are the random variables whose pdf is equal to a Gaussian with variance equal to another variable x_t . We define another random variable z such that, $z_i^2 = x_i^2 - y_i$, where we use the fact that $E[x_i^2] = y_i$ for multiplicative noise. This gives us the expression

$$E[y_{t_1}^2 y_{t_2}^2] = [(z_{t_1}^2 + x_{t_1})(z_{t_2}^2 + x_{t_2})] = E[z_{t_2}^2 z_{t_1}^2 + z_{t_2}^2 x_{t_1} + z_{t_1}^2 x_{t_2} + x_{t_2} x_{t_1}] \quad (18)$$

The middle two terms cancel using the law of total expectations since the expectation of z_i^2 is zero.

$$E[z_{t_2}^2 x_{t_1}] = E[E[z_{t_2}^2 x_{t_1} | x_{t_1} x_{t_2}]] = E[x_{t_1} E[z_{t_2}^2 | x_{t_1} x_{t_2}]] = 0 \quad (19)$$

This leaves us with

$$g_y^2(t_1, t_2) = E[y_{t_1}^2 y_{t_2}^2] = E[z_{t_2}^2 z_{t_1}^2] + E[x_{t_2} x_{t_1}] \quad (20)$$

We see that the second-order correlation of the multiplicative noise is equal to that of the first-order correlation of the underlying process x and that of a mean zero uncorrelated random variable z .

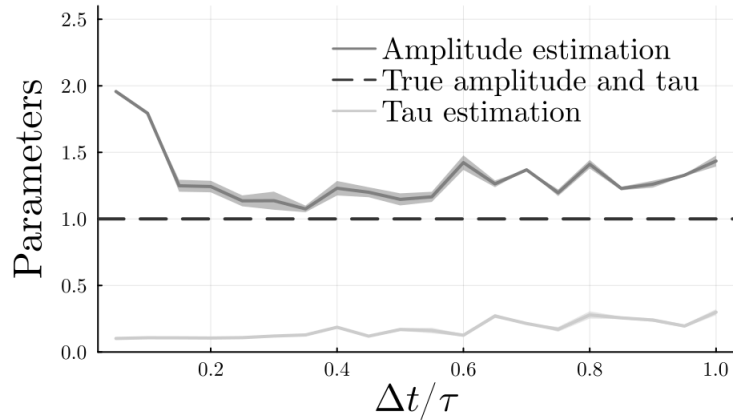


FIG. 3: Parameter estimation for pure multiplicative noise using HMC. We are unable to estimate the true values for the amplitude and tau of the OU signal for any sample rate tested.

Assuming that x_t is an Ornstein-Uhlenbeck process, we can show that the second-order correlation is the same shape as the first-order correlation, and as a result, show that the second-order spectrum of multiplicative noise is hidden by this process. The math is included in the appendix with the final result being

$$g_x^2(t_1, t_2) = \frac{\sigma^4 e^{-2\theta(s+t)}}{2\theta} \left[\frac{3}{2\theta} e^{4\theta \min(s,t)} - 2e^{2\theta \min(s,t)} + 1 + (e^{2\theta \min(s,t)} - 1)(e^{2\theta \max(s,t)} - e^{2\theta \min(s,t)}) \right] + \dots \quad (21)$$

The final result is the sum of exponentials and thus the power spectrum will be the sum of Lorentzian due to the linear properties of the Fourier transform, which have the same general shape as the multiplicative noise previously shown.

In addition, we validated this result in Julia [14] and the results are shown in figure 4, and as shown the multiplicative and OU process share the same underlying shape in the power spectrum, suggesting an explanation for the difficulty in separating the two.

Despite the previous results it is possible to distinguish multiplicative from the signal under certain conditions. Most measurements will have a mixture of both types of noise, and we found that if the ratio of multiplicative to thermal noise is known then it is possible to estimate both the thermal and multiplicative noise.

We define the ratio of thermal to multiplicative noise as,

$$E[x_i^2] \sigma_M^2 / \sigma_N^2 \quad (22)$$

Since the variance of the multiplicative noise is not constant and signal dependant, we use the expectation of the variance of the signal in the following.

This metric allows us to describe the ratio of thermal to multiplicative, and as we will discuss in section III, allows us to correctly fit the amplitudes of both thermal and multiplicative noise, with certain constraints on the ratio of thermal to multiplicative noise.

III. PARAMETER FITTING WITH ADDED MULTIPLICATIVE NOISE

In this section, we employ the Julia programming language [14] to investigate the effectiveness of Hamilton Monte Carlo (HMC) and probabilistic programming in distinguishing multiplicative and thermal noise from an Ornstein-Uhlenbeck (OU) signal. Our fitting algorithm involves generating an OU time series contaminated with thermal and multiplicative noise, followed by using the No U-Turn Sampler (NUTS) and the probabilistic programming package Turing.jl [15] to sample the posterior distribution. We assume uniform prior distributions for all parameters. More details on the algorithm and additional plots and data can be found on our GitHub repository.

Our results show that our fitting algorithm struggles to distinguish between the OU process and multiplicative noise for any sampling time. This is likely due to the similar signature of both processes. In contrast, thermal noise is shown

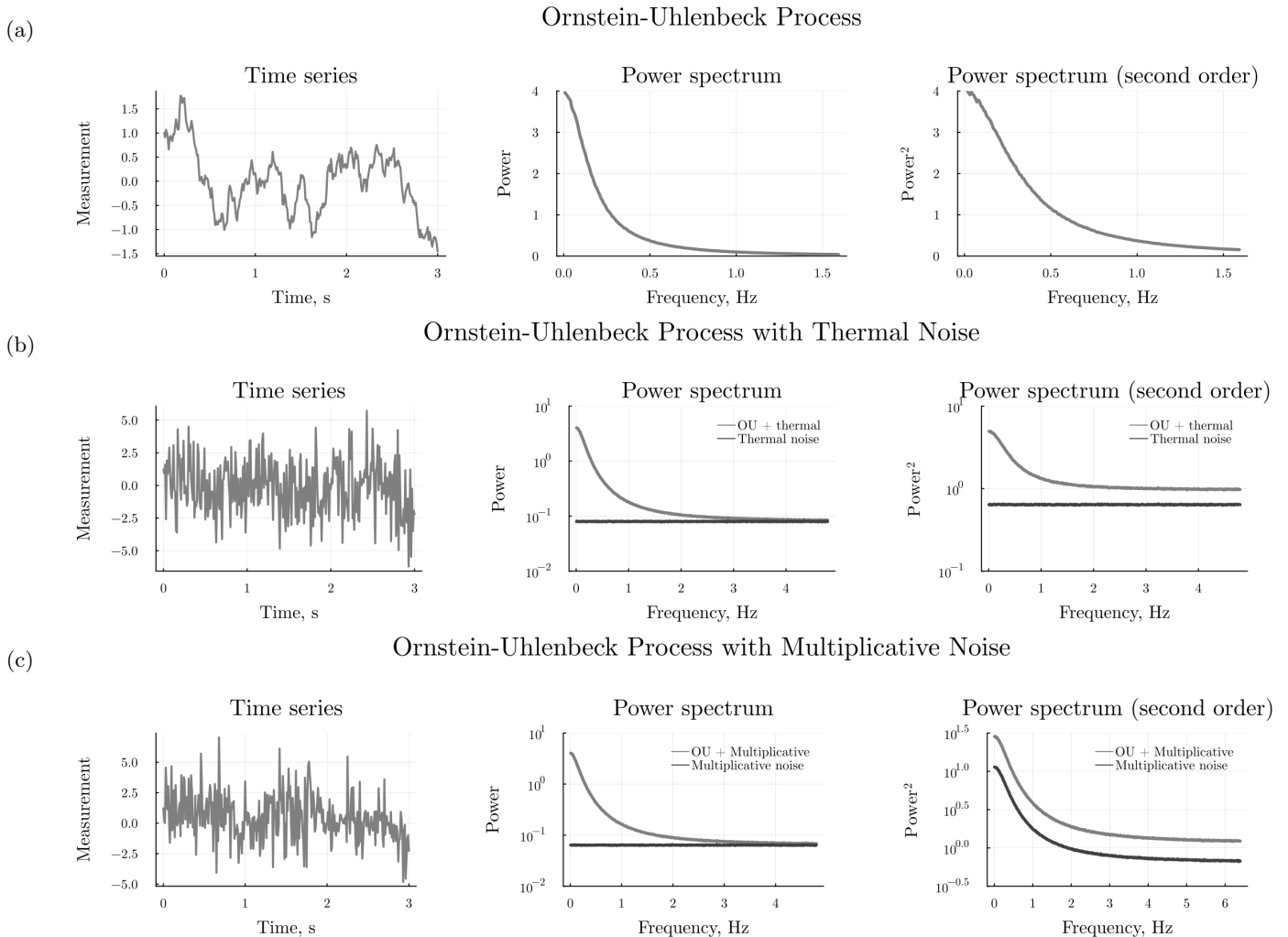


FIG. 4: The above graphs show the power spectrum of the Ornstein-Uhlenbeck process with different types of noise. Figure A is the baseline Ornstein-Uhlenbeck signal. As can be seen, thermal noise (figure B) which is generally easy to subtract is constant in the power spectrum while the multiplicative noise (figure C) closely resembles the Ornstein-Uhlenbeck signal in the second order spectrum, while it looks multiplicative in the first order. For the power spectrum, the curves have been normalized such that the area under the curve is equal to the variance of the signal. For the second-order power spectrum, this is equivalent to the variance of the signal squared.

to be easily distinguishable from the underlying signal when sampling below the time constant τ . We demonstrate this in figure 4 by applying our algorithm for a range of sampling times, each consisting of 1500 points. The generated OU signals all have zero drift and amplitude and τ equal to one.

From these results it is clear that to separate mixed noise (thermal and multiplicative) from the OU signal, we require additional information. In the following, we assume that we know that ratio of thermal to multiplicative noise. One can imagine experimental scenarios, where one can determine thermal noise and multiplicative noise independently and from that establish its ratio. Often multiplicative noise gets introduced by counting processes (Poisson distributions whose variance is equal to the mean) whereas thermal noise could be introduced by noisy amplifiers. In functional magnetic resonance neuroimaging, for example, it is possible to determine this ratio using a dynamic phantom [17].

We now investigate under what circumstances the fitting algorithm can resolve the signal from thermal and multiplicative noise. From our previous findings we expect that there will be a transition point since pure multiplicative noise cannot be separated, whereas thermal noise is easily separated. Indeed, when we vary the multiplicative to thermal noise ratio, we observe a plateau and transition ratio as illustrated in figure 5.

We find that this plateau and transition ratio depends on the data sampling rate in relationship to the OU relaxation rate τ . This is not surprising since the only way to distinguish an OU process from thermal noise is to sample faster

than the OU relaxation rate (see 2). Once we can distinguish the OU process from thermal noise, we can determine the multiplicative noise from the known ratio of multiplicative to thermal noise, leading to a successful separation of noise from OU signal. In figure 5 we plot the measured OU amplitude (true amplitude is 1) versus the ratio of multiplicative to thermal noise. For low ratios we observe a plateau of ratios over which the separation of noise and signal is successful. Once we exceed that ratio, the separation fails. When varying the sampling rate given as the ratio of $\delta t/\tau$ we observe that the plateau shrinks as we decrease the sampling rate. It is worth noting that, during all the simulations, fitting with multiplicative noise took substantially longer than with thermal noise when using HMC sampling methods as described earlier.

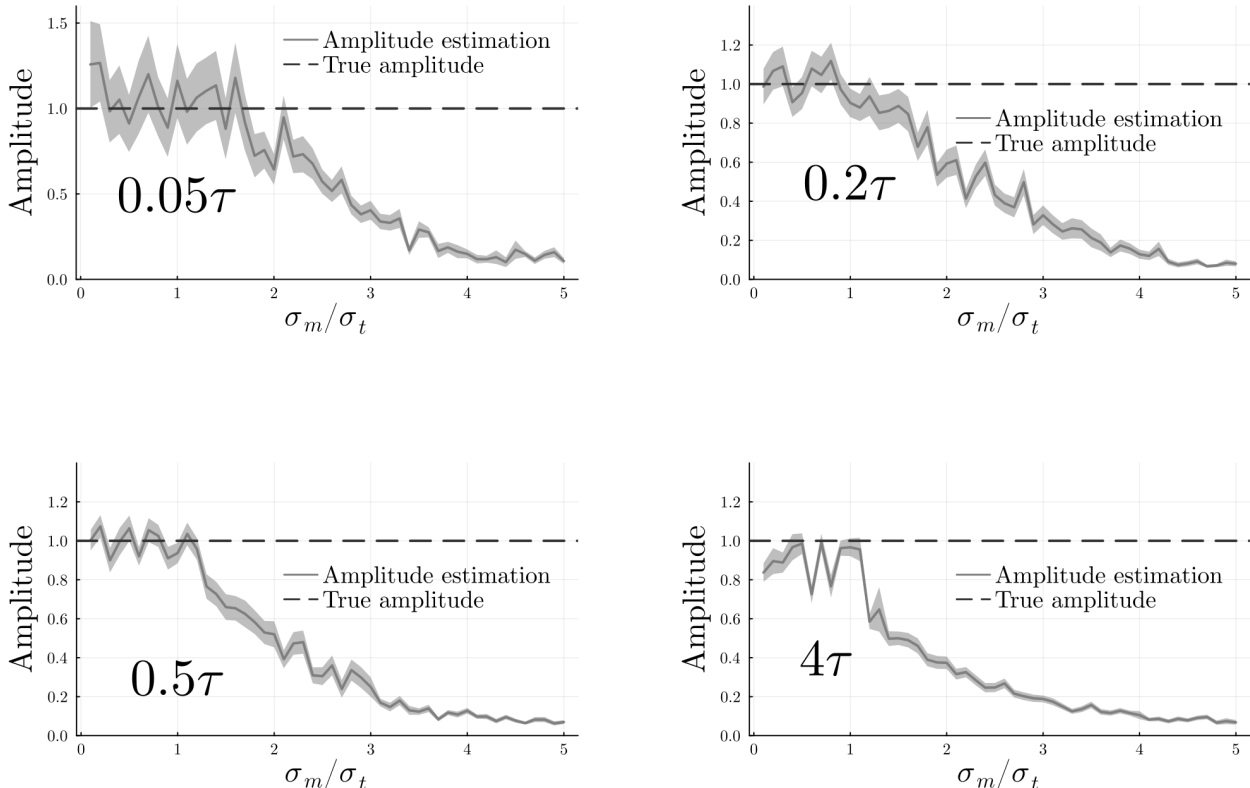


FIG. 5: This is the amplitude estimate for different thermal to multiplicative noise ratios. Each figure represents a different sampling rate from 0.05τ to 4τ , with the true value represented by a dashed line. The total noise is normalized to a magnitude of 0.2 for each ratio. As the ratio of multiplicative to thermal noise increases, we see the amplitude is consistently underestimated, with this effect greater at higher sampling rates

IV. DISCUSSION

In the context of an Ornstein-Uhlenbeck (OU) process, we have developed an efficient algorithm for fitting an OU signal with thermal noise and investigated the properties of multiplicative noise. In cases where the multiplicative signal is insignificant or nonexistent, the expectation maximization (EM) algorithm can be more practical in large-scale simulations. The EM algorithm does not necessarily improve the overall accuracy of the fit compared to HMC, but it can facilitate the analysis of larger datasets, which are increasingly common in biological applications, and pose a struggle for MCMC based simulations [18, 19]. Moreover, the efficiency of the EM algorithm makes it a promising alternative to other approximate generic methods, such as automatic differentiation variational inference (ADVI) [20]. However, the assumption of an underlying OU function with additional uncorrelated noise limits the applicability of our algorithm to a particular class of fitting functions. In addition we can see from Figure 2 that the EM algorithm underestimates the uncertainty of our fit which can lead to unfounded confidence in a particular fit. HMC, on the other hand, is slower but supports a broad range of fitting functions, including those that incorporate multiplicative noise while maintaining more reasonable levels of uncertainty for our parameter estimation. The question then arises regarding how to fit large datasets with multiplicative noise. Our algorithm's effectiveness is due to the OU process's

Gaussian nature and underlying thermal noise, which allows the likelihood to factor. The validity of the model could be further confirmed by comparing it with other approximate methods, such as ADVI. In future research, it would be interesting to explore whether our algorithm can be extended to handle multiplicative noise and be applied to other types of signals as the ability to handle various types of noise will be critical in making accurate predictions in real-world applications.

In situations where the multiplicative noise contribution cannot be approximated by thermal noise, we have demonstrated that HMC struggles to differentiate between multiplicative noise and the underlying signal. Although there is some correlation between the two, it is noteworthy that the similarities are only visible in the second-order power spectrum. This suggests that second-order statistics are inadequate to fully describe the system and that an Ornstein-Uhlenbeck process with multiplicative noise is no longer Gaussian. This issue is especially relevant in fMRI data, where the correlation between brain regions is typically studied, and failure to remove noise results in an underestimation of correlation [21].

The selection of an appropriate sampling rate is a critical factor in experimental settings to minimize noise and effectively distinguish the desired signal. For pure thermal noise, we observe that as the sampling rate increases, we lose the ability to differentiate between thermal noise and the underlying signal. Given a specific time constant, experimenters can use our results to optimize the sampling rate for better data processing. However, with added multiplicative noise, this optimal sampling rate becomes more complex and depends on the ratio of thermal to multiplicative noise within the time series and the number of samples. We discovered that as the ratio of multiplicative noise increases relative to thermal noise, there is a tighter requirement for a higher sampling rate and consequently more samples. This may pose a challenge in certain experiments where there is a limitation on the sampling rate. Nevertheless, we have identified the ideal sampling rates that experimenters can use to extract the best possible data from noise [10].

One possible application arising from our analysis is the use of additional artificial noise to improve the fit. We have shown that HMC fails to distinguish between noise and the signal when the multiplicative noise magnitude exceeds that of the thermal noise. This issue is significant in averaging experiments such as fMRI, where averaging over a particular area of interest may decrease the amount of thermal noise versus multiplicative noise. To address this, it may be possible to add artificial thermal noise to the system, adjusting the noise ratio to a value below one and allowing the removal of multiplicative noise. This could be useful in situations where it was previously impossible to remove multiplicative noise and lead to an increase in the accuracy of further analysis.

A. Appendix

1. Product of two Gaussians

$$\mathcal{N}(x, \mu_1, \sigma_1)\mathcal{N}(x, \mu_2, \sigma_2) \propto \mathcal{N}\left(x, \frac{\mu_1\sigma_2^2 + \mu_2\sigma_1^2}{\sigma_1^2 + \sigma_2^2}, \sqrt{\frac{\sigma_1^2\sigma_2^2}{\sigma_1^2 + \sigma_2^2}}\right) \quad (23)$$

2. Convolution of two Gaussians

$$\int_{-\infty}^{+\infty} \mathcal{N}(x-y, \mu_1, \sigma_1)\mathcal{N}(y, \mu_2, \sigma_2)dy \propto \mathcal{N}\left(x, \mu_1 + \mu_2, \sqrt{\sigma_1^2 + \sigma_2^2}\right) \quad (24)$$

specifically, to calculate $\alpha(x_n)$ and $beta(x_{n-1})$ we encounter the following convolutions

$$\begin{aligned} \int_{-\infty}^{+\infty} dx_{n-1} \exp\left(-\frac{(x_{n-1} - \mu)^2}{2\sigma^2}\right) \exp\left(-\frac{(x_n - Bx_{n-1})^2}{2A(1-B^2)}\right) &\propto \mathcal{N}\left(x_n, B\mu, \sqrt{B^2\sigma^2 + A(1-B^2)}\right) \\ \int_{-\infty}^{+\infty} dx_n \exp\left(-\frac{(x_n - y_n)^2}{2\sigma_N^2}\right) \exp\left(-\frac{(x_n - Bx_{n-1})^2}{2A(1-B^2)}\right) &\propto \mathcal{N}\left(x_{n-1}, y_n/B, \sqrt{\sigma^2 + A(1-B^2)}/B\right) \end{aligned} \quad (25)$$

3. Calculate crosscorrelation coefficients

In Eq. 13 we encounter bivariate distributions such as

$$p(x, y) = \frac{1}{S} \exp\left(-\frac{(x - \mu_x)^2}{2\sigma_x^2}\right) \exp\left(-\frac{(y - Bx)^2}{2A(1 - B^2)}\right) \exp\left(-\frac{(y - \mu_y)^2}{2\sigma_y^2}\right) \quad (26)$$

where S is the normalization constant

$$S = \int_{-\infty}^{\infty} \int_{-\infty}^{\infty} p(x, y) dx dy \quad (27)$$

resulting in the expectation value of xy

$$\begin{aligned} \mathbb{E}(xy) &= \int_{-\infty}^{\infty} \int_{-\infty}^{\infty} p(x, y) xy dx dy \\ &= \frac{1}{(A(1 - B^2) + B^2\sigma_x^2 + \sigma_y^2)^2} \\ &\quad (A(1 - B^2)(B^2\mu_x\mu_y\sigma_x^2 + B\mu_y^2\sigma_x^2 + \mu_x\mu_y\sigma_y^2 + B(\mu_x^2 + \sigma_x^2)\sigma_y^2) \\ &\quad + B(2B\mu_x\mu_y\sigma_x^2)\sigma_y^2 + (\mu_x^2 + \sigma_x^2)\sigma_y^2 + B^2\sigma_x^2(\mu_y^2 + \sigma_y^2)) + A^2(1 - B^2)^2\mu_x\mu_y) \end{aligned} \quad (28)$$

In this section, we collect useful procedures for calculating the different steps in the EM algorithm.

4. OU Second Order Power Spectrum Shape Derivation

We begin by expanding the definition of the second-order power spectrum for our system with multiplicative noise.

$$\begin{aligned} E[(X_1 + Y_1)^2(X_2 + Y_2)^2] &= E[X_1^2X_2^2 + X_1^2Y_2^2 + 2X_2Y_2X_1^2 \\ &\quad + Y_1^2X_2^2 + Y_1^2Y_2^2 + 2X_2Y_2Y_1^2 + 2X_1Y_1X_2^2 + 2X_1Y_1Y_2^2 + 4X_1X_2Y_1Y_2] \end{aligned} \quad (29)$$

Because of the symmetry in all the odd-powered terms, the expectation will be zero, and will not contribute to the autocorrelation function when $t_1 \neq t_2$. For our purposes, since we are interested in an underlying shape we can examine the simplified expression, $E[X_1^2X_2^2]$.

We now enforce the assumption that X_1 and X_2 represent the distribution of an OU process at two different times. It is known that the integral of Brownian motion is equivalent to a zero mean Gaussian with variance (insert citation here),

$$\int_0^t g(s) dW_s = N(0, \int_0^t g(s)^2 ds) \quad (30)$$

The Ornstein-Uhlenbeck process with zero drift is

$$x_t = x_0 e^{-\theta t} + \sigma \int_0^t e^{\theta(t-s)} dW_s \quad (31)$$

For our purposes, we demean and thus we can write,

$$E[x_s^2 x_t^2] = \sigma^4 e^{-2\theta(s+t)} E\left[\left(\int_0^s e^{\theta(u-s)} dW_u\right)^2 \left(\int_0^t e^{\theta(v-t)} dW_v\right)^2\right] \quad (32)$$

assuming $s < t$ we can expand the product as

$$x_s^2 x_t^2 = \sigma^4 e^{-2\theta(s+t)} \left[E\left[\left(\int_0^s e^{\theta(u)} dW_u\right)^4\right] + E\left[\left(\int_0^s e^{\theta(u)} dW_u\right)^2\right] E\left[\left(\int_s^t e^{\theta(v)} dW_v\right)^2\right] \right] \quad (33)$$

we apply Ito-symmetry to the right 2 terms and use equation 24 for the first term producing,

$$x_s^2 x_t^2 = \sigma^4 e^{-2\theta(s+t)} [E[N(0, \int_0^s e^{2\theta u} du)] + \int_0^s e^{2\theta u} du + \int_s^t e^{2\theta v} dv] \quad (34)$$

evaluating the integrals and using the fact that the fourth moment of a Gaussian is $3\sigma^4$ we arrive at the expression

$$g_x^2(s, t_2) = \frac{\sigma^4 e^{-2\theta(s+t)}}{2\theta} \left[\frac{3}{2\theta} e^{4\theta \min(s,t)} - 2e^{2\theta \min(s,t)} + 1 + (e^{2\theta \min(s,t)} - 1)(e^{2\theta \max(s,t)} - e^{2\theta \min(s,t)}) \right] \quad (35)$$

where we generalised in terms of $\min(s, t)$ and $\max(s, t)$ as apposed to $s < t$.

ACKNOWLEDGMENTS

Research presented here was funded by the following: National Science Foundation/White House Brain Research Through Advancing Innovative Technologies (BRAIN) Initiative, United States (NSFNCS-FR 1926781) and the Baszucki Brain Research Fund, United States. In addition, we would like to thank Lilianne R. Mujica-Parodi and Jonathan R. Polimeni for valuable discussions.

-
- [1] D. Sivia and J. Skilling, *Data Analysis: A Bayesian Tutorial*, 2nd ed. (Oxford University Press, 2006).
 - [2] C. Bishop, *Pattern Recognition and Machine Learning*, Information Science and Statistics (Springer, New York, 2006) p. 738.
 - [3] A. Hurn, J. Jeisman, and K. Lindsay, *Journal of Financial Econometrics* **5**, 390–455 (2007).
 - [4] G. Uhlenbeck and I. Ornstein, *Phys. Rev.* **36**, 823 (1930).
 - [5] M. Brennan and E. Schwartz, *The Journal of Business* **58**, 135 (1985).
 - [6] M. Kot, *Elements of Mathematical Ecology* (Cambridge Univ. Press, Cambridge, UK, 2001) p. 464.
 - [7] R. A. Maller, G. Müller, and A. Szimayer, “Ornstein–uhlenbeck processes and extensions,” in *Handbook of Financial Time Series*, edited by T. Mikosch, J.-P. Kreiß, R. A. Davis, and T. G. Andersen (Springer Berlin Heidelberg, Berlin, Heidelberg, 2009) pp. 421–437.
 - [8] L. M. Ricciardi and L. Sacerdote, *Biol Cybern* **35**, 1 (1979).
 - [9] A. Isidori, *Nonlinear Control Systems* (Springer, London, UK, 1995) p. 549.
 - [10] H. H. Strey, *Phys Rev E* **100**, 062142 (2019).
 - [11] A. Gelman and D. Rubin, *Statistical Science* **7**, 457 (1992).
 - [12] S. W. Hasinoff, “Photon, poisson noise,” in *Computer Vision: A Reference Guide*, edited by K. Ikeuchi (Springer US, Boston, MA, 2014) pp. 608–610.
 - [13] P. Lánský and L. Sacerdote, *Physics Letters A* **285**, 132 (2001).
 - [14] J. Bezanson, A. Edelman, S. Karpinski, and V. B. Shah, *SIAM review* **59**, 65 (2017).
 - [15] H. Ge, K. Xu, and Z. Ghahramani, in *International Conference on Artificial Intelligence and Statistics, AISTATS 2018, 9-11 April 2018, Playa Blanca, Lanzarote, Canary Islands, Spain* (2018) pp. 1682–1690.
 - [16] M. Hoffman and A. Gelman, *J. of Machine Learning Research* **15**, 1351 (2014).
 - [17] R. Kumar, L. Tan, A. Kriegstein, A. Lithen, J. R. Polimeni, L. R. Mujica-Parodi, and H. H. Strey, *NeuroImage* **227**, 117584 (2021).
 - [18] R. Bardenet, A. Doucet, and C. Holmes, *Journal of Machine Learning Research* **18** (2015).
 - [19] T. J. Sejnowski, P. S. Churchland, and J. A. Movshon, *Nature Neuroscience* **17**, 1440 (2014).
 - [20] A. Kucukelbir, D. Tran, R. Ranganath, A. Gelman, and D. M. Blei, “Automatic differentiation variational inference,” (2016).
 - [21] S. Whitfield-Gabrieli and A. Nieto-Castanon, *Brain Connectivity* **2**, 125 (2012).